

San Diego, CA) antibodies. For intracellular staining of Foxp3, cells were stained using a Foxp3 Staining Buffer set (eBiosciences).

Flow cytometry

The following antibodies were used for flow cytometry: anti-CD4-APC/H7, anti-CD11c-PE/Cy7, anti-major histocompatibility complex (MHC) class II-Pacific Blue, and anti-CD103-APC antibodies (BD Biosciences). Anti-Foxp3-Alexa Fluor 647 antibodies (eBioscience) were also used; conditions were set according to the manufacturer's instructions. Data were acquired using a FACS Cant-2 instrument with Diva software (Becton Dickinson, Franklin Lakes, NJ, USA).

Intestinal tissue explant cultures

Explant culture was performed according to previously published methods with some modifications.^{15,16} Briefly, large intestines were collected, opened longitudinally, washed in PBS to remove contents, and shaken at 110 rpm in RPMI 1640 containing 50 mg/mL gentamicin, 100 U/mL penicillin, 100 mg/mL streptomycin (GIBCO, Carlsbad, CA, USA), and 5 mmol/L ethylenediaminetetraacetic acid for 20 min at 37°C. After removing epithelial cells and fat tissue, intestinal tissue was cut into 10-mm fragments. Tissue fragments were incubated in 0.5 mL RPMI is abbreviation of Roswell Park Memorial Institute medium. Normally, RPMI is used. 1640 supplemented with 50 mg/mL gentamicin, 100 U/mL penicillin, 100 mg/mL streptomycin, and 5% heat-inactivated fetal bovine serum. Supernatants from the tissue fragment incubations were collected after 24 h for cytokine ELISAs (IL-6 and IL-10; R&D Systems), and tissue dry weights were measured.

Intestinal microflora analysis (T-RFLP method)

Analysis of intestinal bacterial flora using mouse fecal specimens was outsourced to Techno Suruga Laboratory (Shizuoka, Japan), where the T-RFLP (terminal restriction fragment length polymorphism) method was used.¹⁷ The details of this method are described in the Data S1.

Microflora transfer

Microflora transfer was performed according to previously published methods, with modifications.¹⁸ Briefly, 6-week-old female mice were treated with a cocktail of antibiotics (0.5 mg/mL vancomycin [Duchefa Biochemie, Haarlem, the Netherlands], 1 mg/mL ampicillin, 1 mg/mL metronidazole, 1 mg/mL neomycin, and 1 mg/mL

gentamicin [Nacalai Tesque, Kyoto, Japan]) in drinking water for 2 weeks. Diluted cecal contents were collected from 8-week-old mice treated with *C. kefyr* or water for 2 weeks. The ceca of control mice or *C. kefyr*-treated mice were dissected and opened, and the contents were transferred to a sterile tube and resuspended in 50 volumes of sterile water. Next, 200 μ L of this suspension was administered to each recipient by oral gavage using a gavage needle for five consecutive days. At 2 days after the final oral gavage, feces were collected for T-RFLP analysis, and mice were immunized for EAE.

Statistical analysis

Statistical analysis of the results was performed by one-way analysis of variance (ANOVA). Repeated measures ANOVA was used to compare the ratio of bacteria in T-RFLP analysis. Differences were considered significant when *P* values were less than 0.05. The data were analyzed using SPSS 14.J. (SPSS, Chicago, IL, USA)

Results

Candida kefyr decreased the susceptibility of mice to EAE

Eighteen types of yeasts that are found in common fermented foods were investigated in this study (Table S1). Because TNF- α is involved in the pathogenesis of intestinal autoimmune diseases^{19,20} and IL-10 is a key anti-inflammatory cytokine involved in the maintenance of intestinal homeostasis,^{21,22} the effects of yeasts on the production of these cytokines by MNCs from intestinal LP were examined. The yeasts were then classified into four groups depending on the pattern of relative cytokine production: high TNF- α /high IL-10, high TNF- α /low IL-10, low TNF- α /high IL-10, and low TNF- α /low IL-10 (data not shown). Eight yeasts representing the four groups were arbitrarily selected, and their effects on EAE model mice were examined. When administered beginning 14 days before immunization with MOG_{35–55}, only *C. kefyr*, which belonged to the low TNF- α /low IL-10 group, significantly ameliorated the clinical severity of EAE symptoms (Fig. 1A). Pathological examinations revealed that the number of infiltrated MNCs into the spinal cords of mice treated with *C. kefyr* was apparently lower than that observed in the control group (Fig. 1B). The significant decrease in the number of infiltrating cells in the *C. kefyr*-treated group was confirmed by semiquantitative analysis (*C. kefyr*: 1.16 ± 0.24 vs. control: 2.07 ± 0.22 ; *P* = 0.010; Fig. 1C). To investigate the effects of *C. kefyr* on systemic inflammation, draining inguinal LNs and cervical LNs harvested on day 8 after

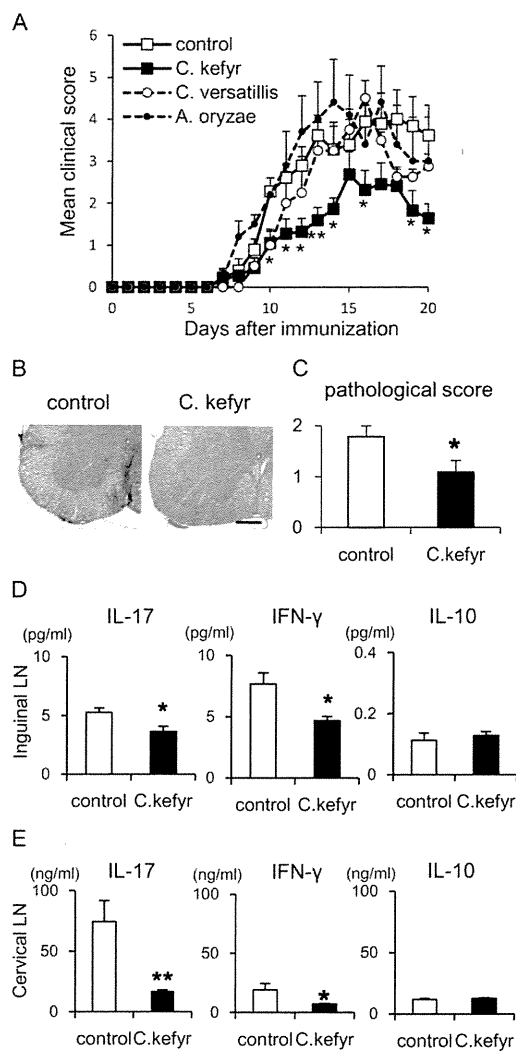


Figure 1. *Candida kefyr* ameliorates symptoms of EAE. The effects of *C. kefyr* ($n = 11$), *C. versatilis* ($n = 8$), *A. oryzae* ($n = 6$), and control (water, $n = 9$) on the clinical severity of EAE are shown. (A) The three yeasts listed above are shown because the other five yeasts did not differ significantly from the control. Yeasts were administered from 14 days before immunization until the end of the study. Data represent the mean clinical score \pm SEM. (* $P < 0.05$, ** $P < 0.01$ compared to the control group using ANOVA). (B) Spinal cord sections obtained from control or *C. kefyr*-treated C57BL/6 mice on day 22 after immunization were analyzed by hematoxylin and eosin (H&E) staining. Scale bar = 250 μ m. (C) Semiquantitative evaluation of the pathological scores was performed as described in the Materials and Methods section. Each bar indicates the mean pathological score \pm SEM of six mice from each group. Lymphocytes were isolated from draining lymph nodes (D) and cervical lymph nodes (E) on day 8 after immunization and then restimulated with MOG_{35–55} for 72 h. IL-17, IFN- γ , and IL-10 in the culture supernatants were assayed by ELISA. Data are means \pm SEMs and are representative of three independent experiments ($n = 5–8$ each). EAE, experimental autoimmune encephalomyelitis; ANOVA, analysis of variance; MOG, myelin oligodendrocyte glycoprotein; IL, interleukin; IFN, interferon; ELISA, enzyme-linked immunosorbent assay.

immunization were restimulated with MOG_{35–55}. Both inguinal and cervical LNs obtained from the *C. kefyr*-treated mice produced significantly less IL-17 and IFN- γ than those obtained from the control group. The production of IL-10 did not differ significantly between the two groups (Fig. 1D and E). Although we assayed IL-4 to examine the effects of *C. kefyr* on Th2-skewing, the levels were below the sensitivity of the assay system. These data suggested that treatment with *C. kefyr* inhibited the induction of antigen-specific Th17 and Th1 cells.

Next, the effects of *C. kefyr* were examined in a model of dextran sulfate sodium (DSS)-induced colitis because inflammatory bowel disease is known to be directly affected by intestinal microflora and intestinal immunity.²³ In this colitis model, prophylactic oral administration of *C. kefyr* significantly inhibited body weight loss, reduced colon length, and increased relative colon weights (Fig. S1A–D). The effects of other *Candida* species were less prominent than those of *C. kefyr*, and no significant differences were observed compared to the control. The effects of *C. kefyr* were also examined in a toluene-2, 4-diisocyanate (TDI) contact dermatitis model, another model of autoimmune dysfunction. However, *C. kefyr*, as well as the other yeasts examined (*C. versatilis*, *C. valida*, and *Saccharomyces cerevisiae*), had no effects on TDI-induced dermatitis (Fig. S2). Thus, our data supported that *C. kefyr* ameliorated symptoms of EAE and DSS-induced colitis, but did not affect TDI-induced dermatitis, suggesting that the efficacy was disease specific.

When *C. kefyr* administration was initiated on day 8 after immunization of mice with EAE, clinical severity was not affected (Fig. S3A). Moreover, in the DSS-induced colitis model, disease deterioration was observed when *C. kefyr* was administered after DSS induction (data not shown). Thus, *C. kefyr* was not effective as a therapeutic agent, but exhibited efficacy in the prophylactic/preventive setting.

***Candida kefyr* suppressed generation of Th17 cells and induced production of regulatory T cells (Tregs) and dendritic cells**

In order to elucidate the mechanism through which *C. kefyr* suppressed intestinal and systemic inflammation, we analyzed CD4⁺ T cells from mice treated with *C. kefyr*. Intracellular staining of CD4⁺ T cells from LP and MLNs of mice treated with *C. kefyr* for 2 weeks revealed that CD4⁺ IL-17-producing cells were downregulated in intestinal LP in both small and large intestines (Fig. 2A). The production of IL-6 by intestinal tissue explants was also downregulated in both small and large intestines, and IL-10 was significantly upregulated in the colon (Fig. 2B). Significantly increased percentages of CD4⁺ Foxp3⁺ iTregs

were observed in *C. kefyr*-treated mice (*C. kefyr*: $7.5 \pm 0.4\%$ vs. control: $9.8 \pm 0.5\%$), although the ratio of Th17 cells was not altered in MLNs (Fig. 2C). No significant differences in the ratios of iTregs in intestinal LP were observed (data not shown). The percentage of CD103⁺ dendritic cells was significantly increased in MLNs (Fig. 2D) and ILNs (data not shown) on day 8 postimmunization in *C. kefyr*-treated mice, although differences were not observed between the two groups before immunization. These data suggested that *C. kefyr* induced the production of Tregs and dendritic cells and suppressed the production of Th17 cells. Additionally,

decreased IL-6 and increased IL-10 levels may contribute to these effects.

Ingestion of *C. kefyr* altered the intestinal microflora

Because intestinal immune cells are affected by intestinal microbiota,²⁴ the intestinal microflora of mice treated with *C. kefyr*-treated mice for 2 weeks was analyzed using the T-RFLP method. There were no differences in the patterns of microflora between the control and *C. kefyr* groups at baseline (Fig. 3A). One week after

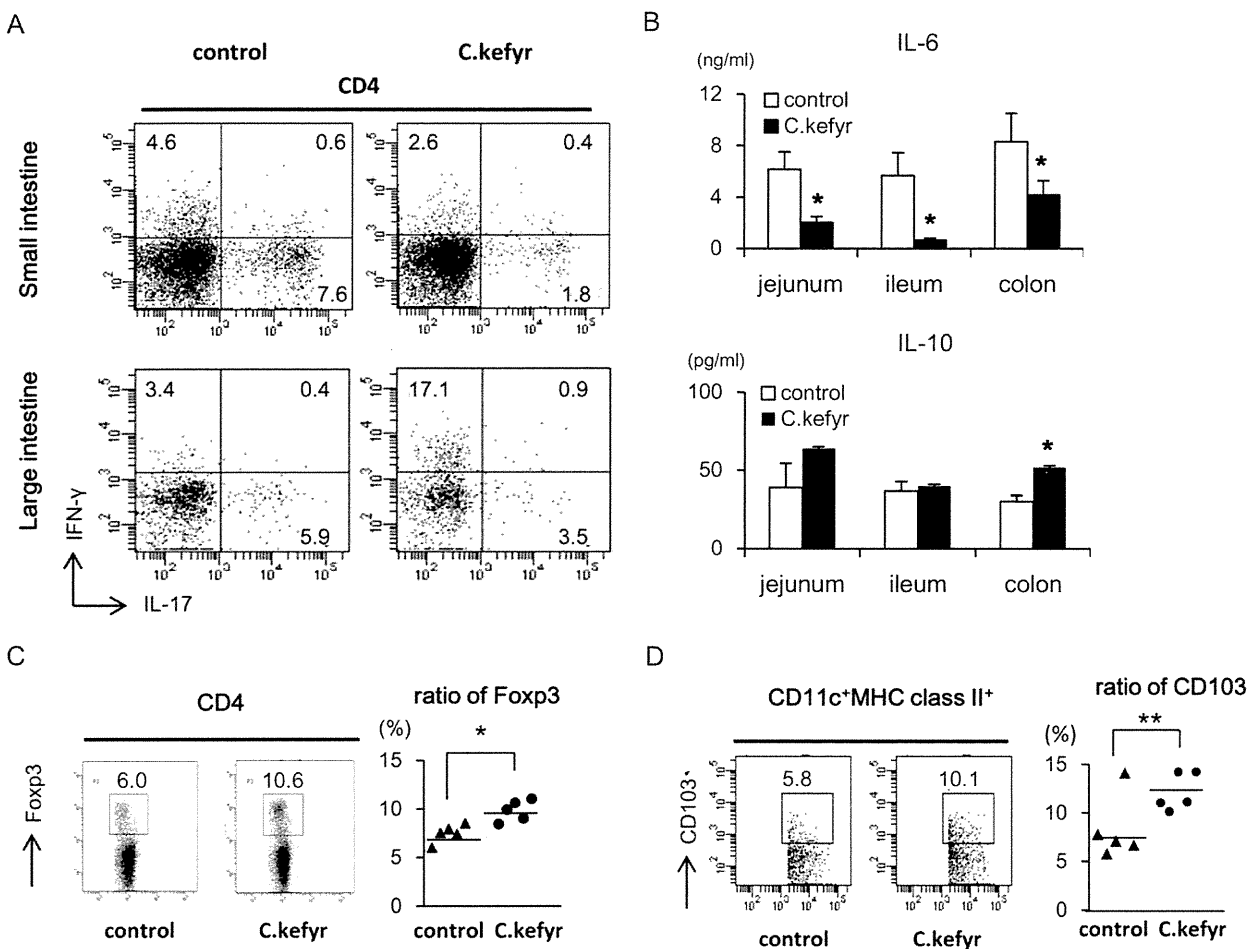


Figure 2. Oral administration of *Candida kefyr* suppresses intestinal Th17 cells and induces regulatory T cells and dendritic cells. (A) Lamina propria lymphocytes from small and large intestines were isolated from *C. kefyr*-treated nonimmunized mice. Intracellular staining of IL-17 and IFN- γ in CD4⁺ T cells was analyzed by flow cytometry. Data are representative of three independent experiments. (B) Tissue explants of small and large intestines from control mice and mice treated with *C. kefyr* for 14 days were cultured for 24 h, and IL-6 and IL-10 in supernatants were assayed by ELISA. (* $P < 0.05$, ** $P < 0.01$ using ANOVA). (C) Lymphocytes from MLNs isolated from *C. kefyr*-treated nonimmunized mice were stained with anti-CD4 and anti-Fopx3 antibodies and analyzed by flow cytometry. Dotplots showed one of five representative experiments, and the graphs show the ratios of Fopx3 cells in CD4⁺ T cells. (D) Lymphocytes from MLNs isolated from *C. kefyr*-treated mice on day 8 postimmunization were stained with anti-CD11c, anti-MHC class II, and anti-CD103 antibodies and analyzed by flow cytometry. Dotplots show one of five representative experiments, and the graphs show the ratio of CD103⁺ cells in CD11c⁺ and MHC class 2⁺ dendritic cells. IL, interleukin; IFN, interferon; ELISA, enzyme-linked immunosorbent assay; MLNs, mesenteric lymph nodes; ANOVA, analysis of variance.

administration, the ratio of *Bacteroides* was decreased in the *C. kefyri*-treated group, while the ratio of *Lactobacillales* remained higher (Fig. 3B). The decrease in the ratio of *Bacteroides* was not observed when administered after immunization (Fig. S3B). In addition to decreased *Bacteroides* and increased *Lactobacillales*, the ratio of *Prevotella* tended to be increased 2 weeks after administration (Fig. 3C). Statistical analysis revealed significantly increased *Lactobacillales* (*C. kefyri*: $49.5 \pm 0.2\%$ vs. control: $24.2 \pm 0.3\%$, $P = 0.005$; Fig. 3D) and significantly decreased *Bacteroides* (*C. kefyri*: $12.6 \pm 5.1\%$ vs. control: $35.6 \pm 6.3\%$, $P = 0.039$; Fig. 3E). *Prevotella* tended to be increased, although the difference was not significant (*C. kefyri*: $16.7 \pm 2.2\%$ vs. control: $10.4 \pm 3.7\%$, $P = 0.325$; Fig. 3F). The percentages of total *Clostridium*, which have been reported to induce regulatory T cells,²⁵ were not different between the two groups (Fig. 3G).

Microflora transferred from *C. kefyri*-treated mice ameliorated symptoms of EAE in recipients

Because *C. kefyri* altered the intestinal microflora, as described above, and therapeutic administration of *C. kefyri* was not effective in either the EAE model or the

DSS-induced colitis model, we hypothesized that modified intestinal microbiota would ameliorate disease pathogenesis and progression. Then, we examined the effects of prophylactic *C. kefyri* administration from day -14 to day 0 postimmunization. Interestingly, this prophylactic administration was still effective, although the effect was less than that of *C. kefyri* administration from day -14 to the end of the study (Fig. 4A). The microflora on day 8 postimmunization exhibited a pattern similar to that observed before EAE induction, as shown in Figures 3C, 4B. Furthermore, CD103-positive DCs were induced in MLNs (Fig. 4C). These results suggested that microflora altered by the ingestion of *C. kefyri* affected the amelioration of EAE.

Thus, we next examined the effects of altered microflora following ingestion of *C. kefyri*. Diluted cecal contents from mice treated with *C. kefyri* for 2 weeks were transferred to recipient mice, and EAE was then induced (Fig. 4D). Analysis of microbiota before immunization showed that the transfer of feces from *C. kefyri*-treated mice tended to decrease *Bacteroides* (*C. kefyri*-t: $7.2 \pm 3.7\%$ vs. control-t: $21.8 \pm 3.6\%$, $P = 0.025$), but did not significantly alter the ratio of *Prevotella* (*C. kefyri*-t: 1.7% vs. control-t: 7.7%) and *Lactobacillales* (*C. kefyri*-t: 25.7% vs. control-t: 23.8%; Fig. 4E and F). The clinical

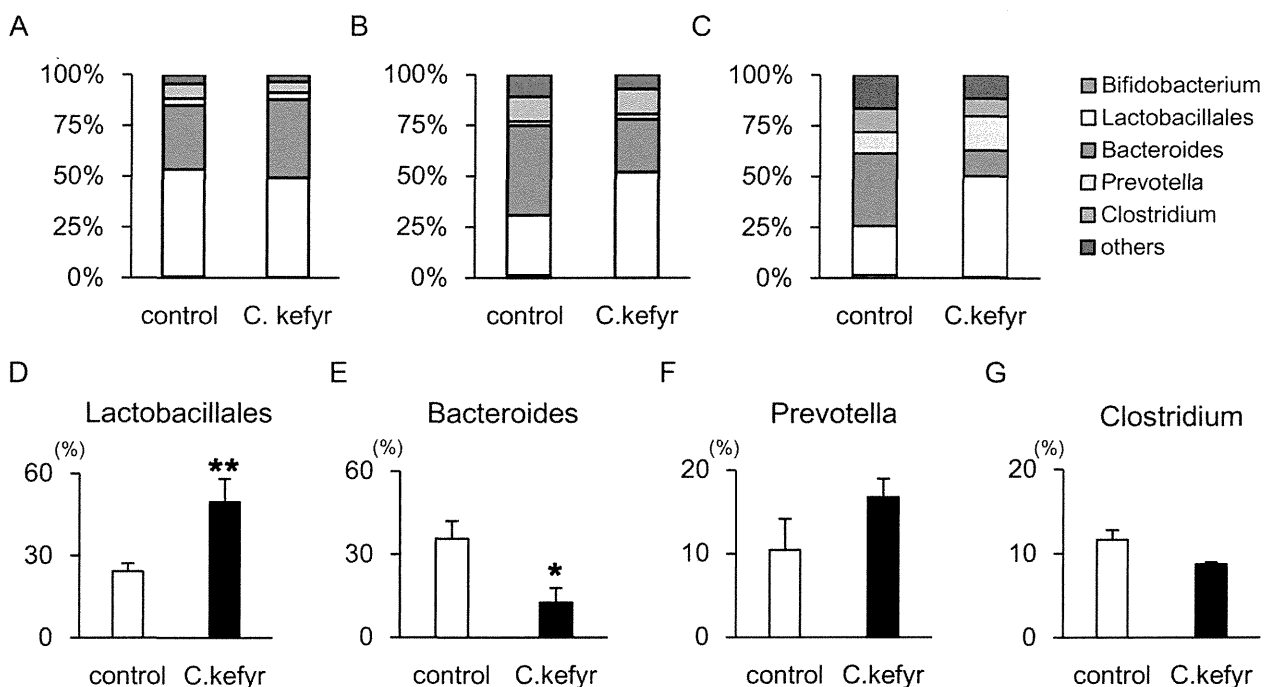


Figure 3. *Candida kefyri* modifies the intestinal microflora. T-RFLP analysis of 16S-rDNA from feces of control mice or mice treated with *C. kefyri*. (A) At baseline (-14 days before immunization [-14 dpi]), (B) 1 week after treatment (-7 dpi), (C) 2 weeks after treatment (day 0). Data show the means of 3–5 mice from two or three independent experiments. (D–G) The ratios of *Lactobacillales*, *Bacteroides*, *Prevotella* and *Clostridium* after a 2-week treatment are shown. Data are the means + SEMs ($n = 5$) (* $P < 0.05$, ** $P < 0.01$ using repeated measures analysis of variance [ANOVA]).

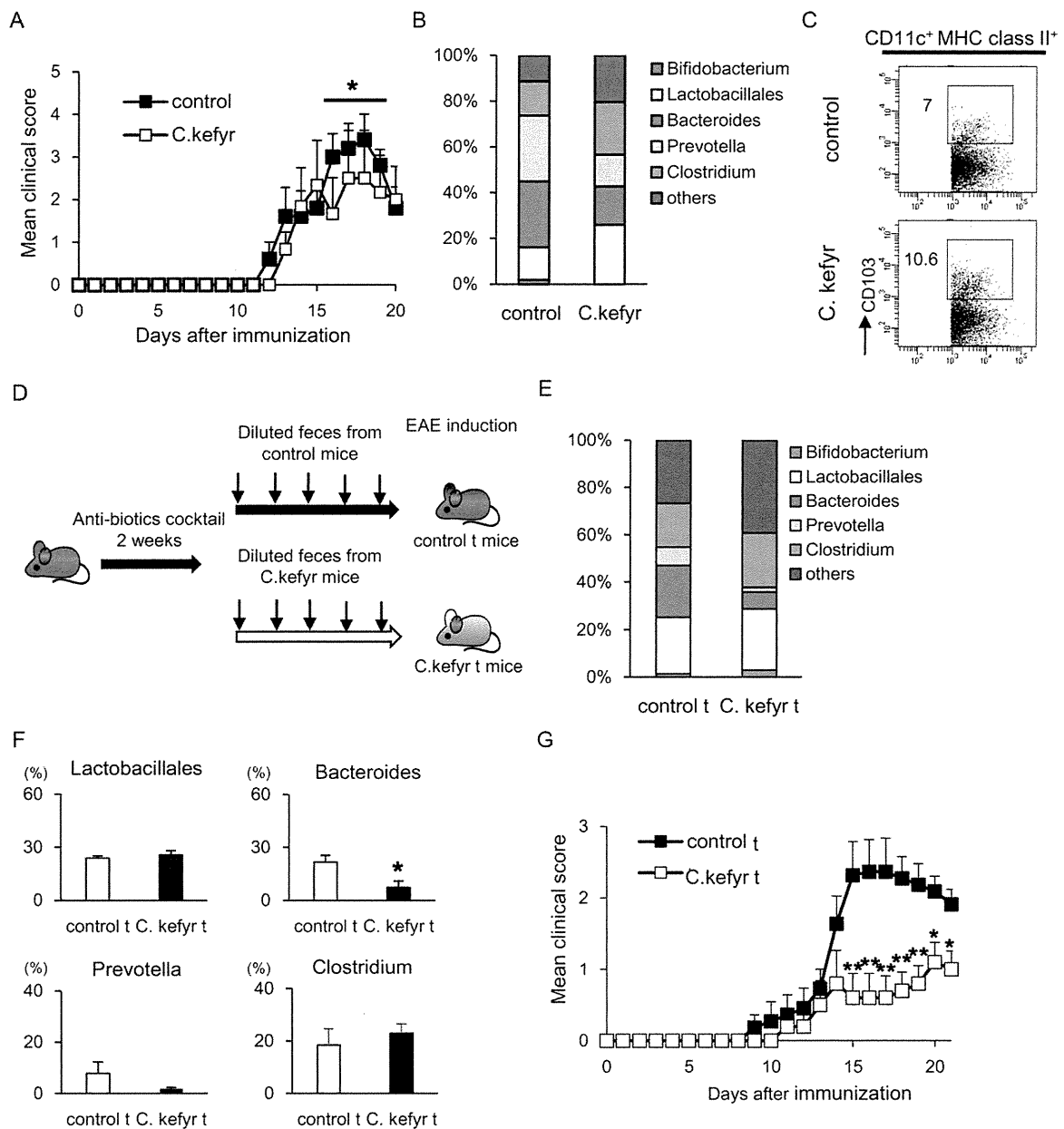


Figure 4. Microflora from *Candida kefyri*-treated mice ameliorates symptoms of EAE. (A) The effects of *C. kefyri* ($n = 6$) administered only prophylactically (from -14 dpi until day 0) and control (water, $n = 6$) on the clinical severity of EAE are shown. Data represent the mean clinical score \pm SEM. The area under the curve (AUC) under the bar was significantly lower in *C. kefyri*-treated mice ($*P < 0.05$ using ANOVA). (B) T-RFLP analysis of 16S-rDNA from feces of control mice or mice treated with *C. kefyri* (from day -14 to day 0) on day 8 postimmunization. (C) Lymphocytes from MLNs isolated from mice treated prophylactically with *C. kefyri* on day 8 postimmunization were stained with anti-CD11c, anti-MHC class II, and anti-CD103 antibodies and analyzed by flow cytometry. Dotplots show one of three representative experiments (D) Schematic of microflora transfer. Mice were treated with an antibiotic cocktail in their drinking water for 2 weeks and were then fed diluted feces from *C. kefyri*-treated mice or control mice once per day for 5 consecutive days. Following a 2-day rest, mice were immunized with MOG₃₅₋₅₅ peptide in CFA. (E) T-RFLP analysis of 16S-rDNA of feces from *C. kefyri*-treated mice and control mice before immunization. Data show the means of five mice from three independent experiments. (F) The ratios of *Lactobacillales*, *Bacteroides*, *Prevotella* and *Clostridium* in 16S-rDNA from feces of control-t or *C. kefyri*-t mice on the day of immunization are shown. Data are the means \pm SEMs ($n = 5$). ($*P < 0.05$, $**P < 0.01$ using repeated measures ANOVA). (G) Clinical scores of EAE mice administered feces from *C. kefyri*-treated (*C. kefyri*-t) or nontreated (control-t) mice. Data show the means \pm SEMs (*C. kefyri*-t, $n = 10$; control-t, $n = 11$) from two independent experiments ($*P < 0.05$ using repeated measures ANOVA). EAE, experimental autoimmune encephalomyelitis; ANOVA, analysis of variance; MLNs, mesenteric lymph nodes; MOG, myelin oligodendrocyte glycoprotein.

scores of mice administered cecal contents from *C. kefyr*-treated mice were significantly decreased compared with those of mice administered cecal contents from control mice (Fig. 4G). Because the microflora of antibiotic-treated recipients before fecal transfer revealed that these four genera were undetectable using the T-RFLP method (data not shown), reconstituted microflora were thought to reflect the original microflora harvested from control or *C. kefyr*-treated mice. In addition, contamination of *C. kefyr* itself or other metabolites was thought to be minimal since the transfer was performed by oral administration of small amount of diluted feces. Taken together, these results suggested that *C. kefyr*-induced changes in microbiota contributed to the amelioration of EAE.

Discussion

Several studies have provided evidence of the importance of microflora in the pathogenesis of multiple sclerosis (MS) pathology,^{2,8,26} and a recent epidemiological analysis conducted in patients living on the island of Crete revealed that modification of microflora due to changes in food habits could be a risk factor for MS.²⁷ In addition, oral administration of a single type of bacterium or a bacterial mixture has been shown to reduce the susceptibility of model animals to EAE.^{10,28–30} However, the effects of yeasts on MS/EAE have not yet been investigated. In the present study, we found that *C. kefyr* had beneficial effects on the symptoms of EAE, suggesting that dietary yeasts prove to be important for the management of immune-mediated diseases.

With regard to the underlying mechanisms, *C. kefyr* treatment was shown to induce CD103⁺ dendritic cells, which function to regulate the immune response, and Foxp3⁺ Tregs in MLNs. Intestinal CD103⁺ dendritic cells are induced by oral administration of polysaccharide A from *Bacteroides fragilis*,^{29,31} while Tregs are induced in MLNs.¹⁰ CD103⁺ dendritic cells migrate towards MLNs in a CCR7-dependent manner.³² In MLNs, CD103⁺ dendritic cells induce Foxp3⁺ Tregs with through a mechanism involving retinoic acid and transforming growth factor (TGF)- β .³³ Our results suggested that induced CD103⁺ dendritic cells have important roles in reducing susceptibility to EAE.

To analyze whether oral administration of *C. kefyr* was effective in other disease models, *C. kefyr* was administered to mice with DSS-induced colitis and TDI contact dermatitis. In the DSS model, colitis is induced by the inflammatory response to microflora.³⁴ Although many types of bacteria have been reported to be effective in the DSS-induced colitis model,³⁵ very few studies have reported the roles of yeasts, such that *Saccharomyces boulardii* that has been shown to reduce the severity of

colitis.³⁶ In the present study, we found that prophylactic administration of *C. kefyr* ameliorated the symptoms of DSS-induced colitis and EAE, but did not affect mice in the TDI dermatitis model, which is induced by a cutaneous delayed-type hypersensitivity response.³⁷ Thus, it seems likely that *C. kefyr* affects some specific immune-mediated diseases, depending on the underlying pathology.

Microflora analysis revealed that ingestion of *C. kefyr* increased *Lactobacillales* and reciprocally decreased *Bacteroides* and increased *Prevotella*. Thus, changes in microflora were identified at the genus level, and the inter-cage effects were minimal within animals in the same group; changes at the species level were not identified due to the limitations of T-RFLP analysis for evaluation of intestinal microflora. Our experiment involving microflora transfer suggested that the decrease in *Bacteroides* rather than the increase in *Lactobacillales* and *Prevotella* seemed to affect the clinical course of EAE. *Bacteroides* and *Prevotella* consist of three predominant enterotypes with Ruminococcus,³⁸ and the reciprocal abundance patterns of these two genera have been reported in several other studies of the human gut microbiome.^{39–41} Consumption of a high-fat diet is known to induce *Bacteroides*, increase intestinal permeability, and promote Th17 immune responses.^{42,43} In our study, ingestion of *C. kefyr* inhibited the production of IL-6 and generation of Th17 cells in intestinal LP in the intestine. Microflora modify local activation of the IL-6 pathway,⁴⁴ and commensal *Bacteroides* species can induce spontaneous inflammatory colitis, depending on the genetic backgrounds.⁴⁵ The present data suggested that modification of the intestinal microflora by *C. kefyr* reduced susceptibility to inflammation by decreasing IL-6 production.

The relationship between intestinal fungi and bacteria is not well understood. One study reported a correlation between intestinal fungi and bacteria, such as *Prevotella* and *Bacteroides*.⁴⁶ *Candida* species have been shown to induce production of carbohydrates, which subsequently reduce the ratio of *Bacteroides*.⁴⁶ In our study, although both *C. kefyr* and *S. cerevisiae* increased the proportion of *Lactobacillus* species, *Saccharomyces* species did not reduce the ratio of *Bacteroides* (data not shown). Thus, *C. kefyr* may have significant effects on the *Bacteroides* ratio through a mechanism that is distinct from that of *S. cerevisiae*.

In conclusion, *C. kefyr* decreased the ratio of *Bacteroides* and the production of IL-6 in the intestines, which contributed in part to the induction of regulatory dendritic cells and the suppression of EAE. Therefore, modulation of microflora by dietary yeasts may be an option to prevent and treat MS.

Author Contribution

K. T. and T. T. carried out the experiments. K. T. and Y. N. wrote the paper. T. K. and J. A. H. assisted the experiments. T. O., M. K., M. T., and T. S. assisted with interpretations of data. S. S. and Y. N. designed the experiments. K. H., H. M., and S. S. supervised the study.

Conflict of Interest

K. T., T. T., T. O., T. K., M. T., K. H., S. S., and Y. N. has a patent (2013-044430) pending relevant to this work. T. T., M. T., and K. H. are relevant persons of Kyorin Pharmaceutical Co., Ltd.

References

- Claesson MJ, Jeffery IB, Conde S, et al. Gut microbiota composition correlates with diet and health in the elderly. *Nature* 2012;488:178–184.
- Lee YK, Menezes JS, Umesaki Y, Mazmanian SK. Proinflammatory T-cell responses to gut microbiota promote experimental autoimmune encephalomyelitis. *Proc Natl Acad Sci USA* 2011;108(suppl 1):4615–4622.
- Korn T, Bettelli E, Oukka M, Kuchroo VK. IL-17 and Th17 Cells. *Annu Rev Immunol* 2009;27:485–517.
- Ivanov II, Atarashi K, Manel N, et al. Induction of intestinal Th17 cells by segmented filamentous bacteria. *Cell* 2009;139:485–498.
- Wu HJ, Ivanov II, Darce J, et al. Gut-residing segmented filamentous bacteria drive autoimmune arthritis via T helper 17 cells. *Immunity* 2010;32:815–827.
- Atarashi K, Tanoue T, Oshima K, et al. Treg induction by a rationally selected mixture of Clostridia strains from the human microbiota. *Nature* 2013;500:232–236.
- Esplugues E, Huber S, Gagliani N, et al. Control of TH17 cells occurs in the small intestine. *Nature* 2011;475:514–518.
- Yokote H, Miyake S, Croxford JL, et al. NKT cell-dependent amelioration of a mouse model of multiple sclerosis by altering gut flora. *Am J Pathol* 2008;173:1714–1723.
- Sartor RB. Therapeutic manipulation of the enteric microflora in inflammatory bowel diseases: antibiotics, probiotics, and prebiotics. *Gastroenterology* 2004;126:1620–1633.
- Takata K, Kinoshita M, Okuno T, et al. The lactic acid bacterium *Pediococcus acidilactici* suppresses autoimmune encephalomyelitis by inducing IL-10-producing regulatory T cells. *PLoS One* 2011;6:e27644.
- Di Giacinto C, Marinaro M, Sanchez M, et al. Probiotics ameliorate recurrent Th1-mediated murine colitis by inducing IL-10 and IL-10-dependent TGF-beta-bearing regulatory cells. *J Immunol* 2005;174:3237–3246.
- Wyder MT, Meile L, Teuber M. Description of *Saccharomyces turicensis* sp. nov., a new species from kefir. *Syst Appl Microbiol* 1999;22:420–425.
- Lee MY, Ahn KS, Kwon OK, et al. Anti-inflammatory and anti-allergic effects of kefir in a mouse asthma model. *Immunobiology* 2007;212:647–654.
- Kinoshita M, Nakatsuji Y, Kimura T, et al. Neuromyelitis optica: passive transfer to rats by human immunoglobulin. *Biochem Biophys Res Commun* 2009;386:623–627.
- Kang S, Okuno T, Takegahara N, et al. Intestinal epithelial cell-derived semaphorin 7A negatively regulates development of colitis via alphavbeta1 integrin. *J Immunol* 2012;188:1108–1116.
- Hegazi RA, Rao KN, Mayle A, et al. Carbon monoxide ameliorates chronic murine colitis through a heme oxygenase 1-dependent pathway. *J Exp Med* 2005;202:1703–1713.
- Oda Y, Ueda F, Kamei A, et al. Biochemical investigation and gene expression analysis of the immunostimulatory functions of an edible Salacia extract in rat small intestine. *Biofactors* 2011;37:31–39.
- Markle JG, Frank DN, Mortin-Toth S, et al. Sex differences in the gut microbiome drive hormone-dependent regulation of autoimmunity. *Science* 2013;339:1084–1088.
- Baumgart DC, Carding SR. Inflammatory bowel disease: cause and immunobiology. *Lancet* 2007;369:1627–1640.
- Rutgeerts P, Sandborn WJ, Feagan BG, et al. Infliximab for induction and maintenance therapy for ulcerative colitis. *N Engl J Med* 2005;353:2462–2476.
- Izcue A, Coombes JL, Powrie F. Regulatory lymphocytes and intestinal inflammation. *Annu Rev Immunol* 2009;27:313–338.
- Wagener J, Malireddi RK, Lenardon MD, et al. Fungal chitin dampens inflammation through IL-10 induction mediated by NOD2 and TLR9 activation. *PLoS Pathog* 2014;10:e1004050.
- Fuhrer A, Sprenger N, Kurakevich E, et al. Milk sialyllactose influences colitis in mice through selective intestinal bacterial colonization. *J Exp Med* 2010;207:2843–2854.
- Ivanov II, Honda K. Intestinal commensal microbes as immune modulators. *Cell Host Microbe* 2012;12:496–508.
- Atarashi K, Tanoue T, Shima T, et al. Induction of colonic regulatory T cells by indigenous Clostridium species. *Science* 2011;331:337–341.
- Berer K, Mues M, Koutrolos M, et al. Commensal microbiota and myelin autoantigen cooperate to trigger autoimmune demyelination. *Nature* 2011;479:538–541.
- Kotzamani D, Panou T, Mastorodemos V, et al. Rising incidence of multiple sclerosis in females associated with urbanization. *Neurology* 2012;78:1728–1735.
- Ezendam J, de Klerk A, Gremmer ER, van Loveren H. Effects of *Bifidobacterium animalis* administered during

- lactation on allergic and autoimmune responses in rodents. *Clin Exp Immunol* 2008;154:424–431.
29. Ochoa-Reparaz J, Mielcarz DW, Wang Y, et al. A polysaccharide from the human commensal *Bacteroides fragilis* protects against CNS demyelinating disease. *Mucosal Immunol* 2010;3:487–495.
 30. Lavasani S, Dzhambazov B, Nouri M, et al. A novel probiotic mixture exerts a therapeutic effect on experimental autoimmune encephalomyelitis mediated by IL-10 producing regulatory T cells. *PLoS One* 2010;5:e9009.
 31. Ochoa-Reparaz J, Mielcarz DW, Ditrio LE, et al. Central nervous system demyelinating disease protection by the human commensal *Bacteroides fragilis* depends on polysaccharide A expression. *J Immunol* 2010;185:4101–4108.
 32. Schulz O, Jaensson E, Persson EK, et al. Intestinal CD103+, but not CX3CR1+ antigen sampling cells migrate in lymph and serve classical dendritic cell functions. *J Exp Med* 2009;206:3101–3114.
 33. Coombes JL, Siddiqui KR, Arancibia-Carcamo CV, et al. A functionally specialized population of mucosal CD103+ DCs induces Foxp3+ regulatory T cells via a TGF- β and retinoic acid-dependent mechanism. *J Exp Med* 2007;204:1757–1764.
 34. Perse M, Cerar A. Dextran sodium sulphate colitis mouse model: traps and tricks. *J Biomed Biotechnol* 2012;2012:718617.
 35. Nanau RM, Neuman MG. Nutritional and probiotic supplementation in colitis models. *Dig Dis Sci* 2012;57:2786–2810.
 36. Chen X, Yang G, Song JH, et al. Probiotic yeast inhibits VEGFR signaling and angiogenesis in intestinal inflammation. *PLoS One* 2013;8:e64227.
 37. Fuchibe K, Nabe T, Fujii M, et al. Delayed type allergic itch-associated response induced by toluene-2,4-diisocyanate in hairless mice. *J Pharmacol Sci* 2003;93:47–54.
 38. Arumugam M, Raes J, Pelletier E, et al. Enterotypes of the human gut microbiome. *Nature* 2011;473:174–180.
 39. Tyakht AV, Kostyukova ES, Popenko AS, et al. Human gut microbiota community structures in urban and rural populations in Russia. *Nat Commun* 2013;4:2469.
 40. Yatsunenkov T, Rey FE, Manary MJ, et al. Human gut microbiome viewed across age and geography. *Nature* 2012;486:222–227.
 41. De Filippo C, Cavalieri D, Di Paola M, et al. Impact of diet in shaping gut microbiota revealed by a comparative study in children from Europe and rural Africa. *Proc Natl Acad Sci USA* 2010;107:14691–14696.
 42. Wu GD, Chen J, Hoffmann C, et al. Linking long-term dietary patterns with gut microbial enterotypes. *Science* 2011;334:105–108.
 43. Gruber L, Kisling S, Lichti P, et al. High fat diet accelerates pathogenesis of murine Crohn's disease-like ileitis independently of obesity. *PLoS One* 2013;8:e71661.
 44. Hu B, Elinav E, Huber S, et al. Microbiota-induced activation of epithelial IL-6 signaling links inflammasome-driven inflammation with transmissible cancer. *Proc Natl Acad Sci USA* 2013;110:9862–9867.
 45. Bloom SM, Bijanki VN, Nava GM, et al. Commensal *Bacteroides* species induce colitis in host-genotype-specific fashion in a mouse model of inflammatory bowel disease. *Cell Host Microbe* 2011;9:390–403.
 46. Hoffmann C, Dollive S, Grunberg S, et al. Archaea and fungi of the human gut microbiome: correlations with diet and bacterial residents. *PLoS One* 2013;8:e66019.

Supporting Information

Additional Supporting Information may be found in the online version of this article:

Table S1. Dietary yeasts examined in this study.

Figure S1. *Candida kefyr* administration ameliorates DSS-induced colitis. Yeasts (*C. kefyr*, $n = 10$; *C. versatilis*, $n = 10$; *C. valida*, $n = 9$) or water ($n = 10$) were administered to C57BL/6 mice in a water bottle for 14 days before DSS administration. (A) Percent weight change after DSS administration for 5 days. The initial weight of each mouse was defined as 100%. Data are representative of two independent experiments. Each bar indicates the mean body weight (%) \pm SEM. ($*P < 0.05$ compared to the control group using ANOVA). (B) Colon length and (C) relative weight of the colon collected on day 20 after DSS treatment. The sums of two experiments are shown. Each bar represents the mean \pm SEM (*C. kefyr*, $n = 20$; *C. versatilis*, $n = 20$; *C. valida*, $n = 19$; water, $n = 20$). ($*P < 0.05$, $**P < 0.01$ using ANOVA). (D) Colon sections obtained from control or *C. kefyr*-treated C57BL/6 mice on day 18 after DSS treatment were analyzed by hematoxylin and eosin (H&E) staining. Scale bar = 200 μ m. Data are representative of four mice from two independent experiments.

Figure S2. The effects of yeast administration in the TDI model. Seven-week-old BALB/c mice were administered water ($n = 9$) or yeasts (*Candida kefyr*, *C. versatilis*, *C. valida*, and *Saccharomyces cerevisiae* 0.8 mg/mL) in a water bottle beginning 2 weeks before TDI sensitization to the end of the study. Application of TDI to mouse ears was performed 3 weeks after preapplication of TDI to bilateral hind legs. Increases in ear thickness were measured 22 and 48 h after the second application. Data are representative of two experiments and are presented as the mean clinical score.

Figure S3. Therapeutic administration of *Candida kefyr* does not ameliorate EAE. The effects of therapeutic administration of *C. kefyr* ($n = 6$) and control (water, $n = 6$) on the clinical severity of EAE are shown. (A) *Candida kefyr* was administered from the day of clinical onset until the end of the study. Data represent the mean

clinical score \pm SEM. (B) T-RFLP analysis of 16s-rDNA from feces of control mice or mice treated with *C. kefyr* from the day after immunization to day 7 after treatment. Representative data of three independent experiments are shown.

Data S1. Supplementary methods.

Research Article

Parkinsonian Rigidity Depends on the Velocity of Passive Joint Movement

Takuyuki Endo,¹ Naoya Yoshikawa,² Harutoshi Fujimura,¹ and Saburo Sakoda¹

¹Department of Neurology, Toneyama National Hospital, 5-1-1 Toneyama, Toyonaka, Osaka 560-8552, Japan

²Graduate School of Engineering Science, Osaka University, 1-3 Machikaneyama, Toyonaka, Osaka 560-8531, Japan

Correspondence should be addressed to Takuyuki Endo; tendo@toneyama.go.jp

Received 5 July 2015; Accepted 7 December 2015

Academic Editor: Ivan Bodis-Wollner

Copyright © 2015 Takuyuki Endo et al. This is an open access article distributed under the Creative Commons Attribution License, which permits unrestricted use, distribution, and reproduction in any medium, provided the original work is properly cited.

Background. It has been long believed that Parkinsonian rigidity is not velocity-dependent based on the neurological examination. However, this has not been verified scientifically. **Methods.** The elbow joints of 20 Parkinson's disease patients were passively flexed and extended, and two characteristic values, the elastic coefficient (elasticity) and the difference in bias (difference in torque measurements for extension and flexion), were identified from a plot of the angle and torque characteristics. Flexion and extension were done at two different velocities, 60°/s and 120°/s, and a statistical analysis was performed to determine whether the changes in these characteristic values were velocity-dependent. **Results.** The elastic coefficient was not velocity-dependent, but the difference in bias increased in a velocity-dependent manner ($P = 0.0017$). **Conclusions.** The features of rigidity may differ from the conventional definition, which states that they are not dependent on the velocity of joint movement.

1. Introduction

Rigidity and spasticity are two well-known abnormalities of muscle tone. Rigidity is a major characteristic of Parkinson's disease (PD), and it has been distinguished from spasticity in that the resistance of a joint is typically described as constant regardless of the joint angle and is not dependent on the velocity of the movement [1]. (We regard “velocity” as “angular velocity” in this report.) However, such a definition depends on the subjective method of neurological examination, and it should be confirmed by a scientific measurement system. With respect to rigidity in PD patients, Lee et al. quantified the velocity-dependent features of muscle tone using a torque meter when the elbow was flexed at a constant speed, and they showed velocity dependence [2]. However, they did not show that the characteristic values used in that study were correlated with rigidity in clinical assessments. The pathophysiology of Parkinsonian rigidity has been investigated using electrophysiological technique for a long time. From the clinical observation of muscular rigidity, many researchers have been interested in the stretch reflex response. They defined the M1 response as a tendon jerk and the M2 response as a long latency stretch reflex,

and the M2 response had twice the tendon jerk latency with a much larger amplitude than the M1 response. Lee and Tatton examined the long latency stretch reflex in wrist flexor muscles of PD patients [3]. They observed an exaggerated M2 response, while the M1 response was unchanged. However, Rothwell et al. measured the long latency stretch reflex in triceps brachii and flexor pollicis longus muscles in PD patients with severe rigidity and showed that the M2 response was greatly increased in triceps brachii, whereas a normal M2 response was observed in flexor pollicis longus [4]. They concluded that enhanced long latency reflexes contribute to, but may not be solely responsible for, rigidity. Thus which components contribute to rigidity is still unclear. Activation rigidity, which is the clinically well-known phenomenon of reinforcing rigidity in one limb by requesting a voluntary flexion or extension in the other limb, is thought to indicate the central nervous system influence in the pathogenesis of rigidity [5]. Although activated rigidity may affect the long latency reflex system, it had not previously been adequately validated in clinical practice.

We previously succeeded in systematically analyzing factors of rigidity perceived by physicians in clinical examinations [6]. The results showed that the elastic coefficient

(elasticity) and the difference in bias (difference in torque during flexion and extension) are factors in rigidity and that rigidity is perceived to be strong when either or both of these factors are large. We then considered the elastic coefficient, one of the component factors of rigidity, not as having one feature over the full joint angle range but as a model combining two elastic characteristics with different features. We previously showed the validity of the technique of analyzing elbow joint movement divided into angles proximal and distal to a joint angle of 60° [7]. In this study, the elbow joints of PD patients were moved passively at different velocities, and two components of rigidity were evaluated to determine whether they were velocity-dependent.

2. Methods

2.1. Subjects. This study included 20 patients (10 men and 10 women; mean age: 74.4 ± 6.2 years) diagnosed with PD according to British Brain Bank clinical criteria [8]. PD patients were assessed using UPDRS (Unified Parkinson Disease Rating Scale) Part III, and rigidity was scored using a five-point scale (0 = no rigidity, 1 = slight, 2 = mild to moderate, 3 = marked, and 4 = severe). The rigidity detected only during activation was not rated as score 1 or 0, because the patients were instructed to remain relaxed during the measurement and no movement was induced. The upper limb of the side that showed more severe rigidity was analyzed in each subject; it was the left side in 16 patients and the right side in 4 patients. In the present study, the UPDRS rigidity score was 1 in 8 patients, 2 in 9 patients, and 3 in 3 patients. All patients were on medication during the UPDRS assessment and during the measurements. All of the present subjects underwent head MRI, but no central nervous system lesions that would cause spasticity in the arms were seen. This study was approved by the Institutional Review Board of Toneyama National Hospital, and written, informed consent was obtained from all subjects in accordance with the Declaration of Helsinki.

2.2. Muscle Tone Measurement Device and Protocols. Figure 1 shows an overview of the muscle tone measurement system and the measurement protocol. This device consisted of small 3-axis force sensors and a gyro sensor. Two force sensors with soft pads were placed on either side of the wrist joint to measure the force perpendicular to the long axis of the arm during flexion and extension movements of the elbow joint and to calculate the torque at the elbow joint. The signals from the gyro sensor attached between the force sensors were used to calculate the angle of the elbow joint. The subjects were instructed to remain relaxed in the sitting position. An examiner held the elbow joint of the subject with one hand and the wrist joint of the subject with the other hand and performed passive flexion and extension of the elbow joint of the subject. The measurement was started from the maximum extension position. The following movements were repeated over 60 sec: more than 3 sec rest, flexion over 2 sec, more than 3 sec rest at the maximum flexion position, extension over 2 sec, and more than 3 sec rest at the maximum

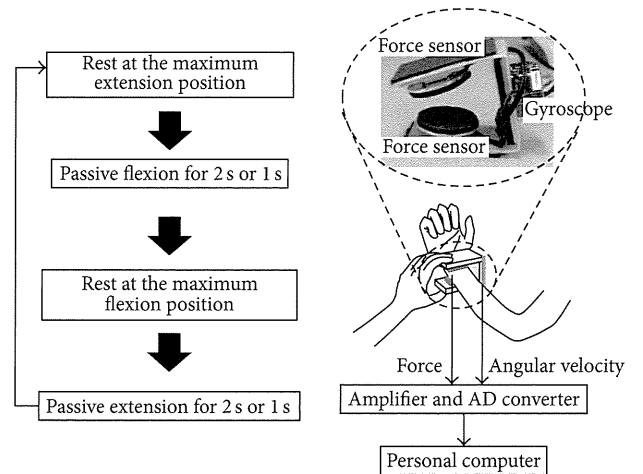


FIGURE 1: Overview of the muscle tone measurement system and the measurement protocol.

extension position. Each trial included five cycles of flexion and extension, and the times for flexion and extension were one time each for 2 sec ($60^\circ/s$) and 1 sec ($120^\circ/s$).

2.3. Data Analysis

- (1) Two different characteristic values, the elastic coefficient and the difference in bias, were extracted from the angle-torque characteristic plots during elbow flexion and extension in 20 PD patients. The angle-torque characteristic plots of one PD patient (UPDRS rigidity score = 3) were shown in Figure 2.
- (2) Elastic coefficient: the data for joint angles of $10\text{--}110^\circ$ were taken from the graphs of angle-torque characteristics of the elbow because inertial force may affect the data in the beginning and ending of the flexion and extension phase. The elastic coefficient was calculated by obtaining the slopes of the respective regression lines for flexion and extension.
- (3) Difference in bias: bias was first defined as the torque value during flexion at one joint angle. It was defined similarly during extension. The difference in bias during flexion and extension was then calculated for the three angles of 30° , 60° , and 90° , and these values were summed.
- (4) Statistical analysis: the elastic coefficients and the difference in bias, which were the characteristic values of muscle tone for the 20 PD patients, were analyzed statistically to determine whether there was velocity dependence in flexion and extension (JMP 11, SAS Institute Inc., Cary, NC, USA). Ten measurements, including five repetitive tests at two velocities, $60^\circ/s$ and $120^\circ/s$, were recorded for each subject. Mixed-design analysis of variance for repeated measures was used for comparisons between the measurements of two velocities. Multivariate F tests were used because the sphericity chi-square test was significant.

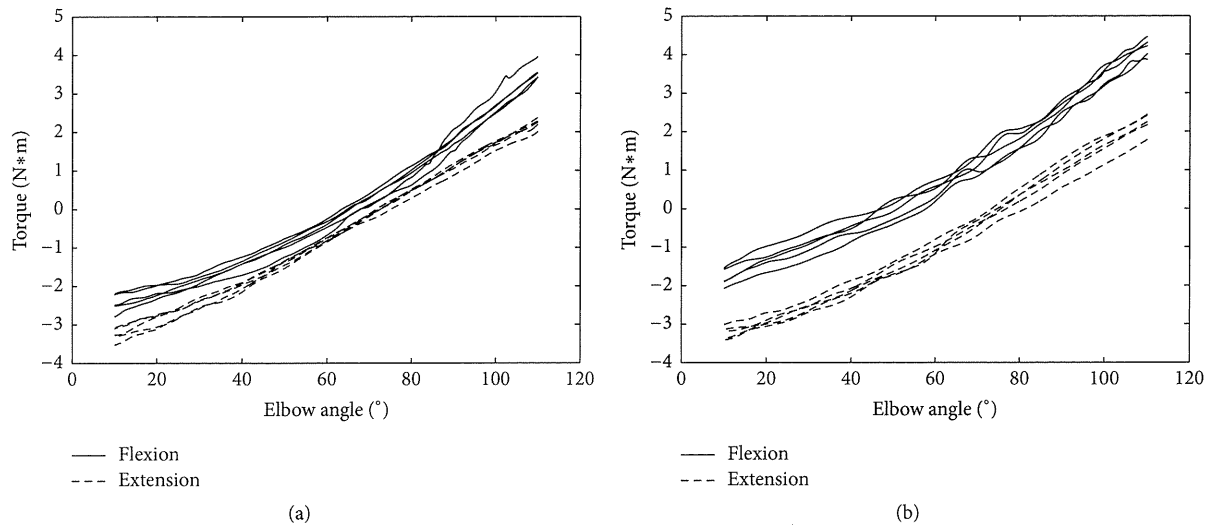


FIGURE 2: Angle-torque characteristics in passive flexion (solid line) and passive extension (dashed line) of left upper limb in one PD patient (UPDRS rigidity score = 3). The data included five cycles in (a) angular velocity $60^\circ/\text{s}$ and (b) angular velocity $120^\circ/\text{s}$.

3. Results and Discussion

As shown in Figure 3, there was no difference in the elastic coefficient between the two velocities of $60^\circ/\text{s}$ and $120^\circ/\text{s}$ during extension ($P = 0.6679$) and flexion ($P = 0.5924$). In contrast, a significant velocity dependence was seen in a comparison of the sum of the differences in bias at $60^\circ/\text{s}$ with that at $120^\circ/\text{s}$ ($P = 0.0017$). The sum of the differences in bias increased as the velocity increased. The elastic coefficient and the difference in bias are two components of Parkinsonian rigidity, but they might have different features; the elastic coefficient has positional dependence as it is defined, and the difference in bias has velocity dependence.

The present result is the first to show velocity dependence in one component of rigidity that corresponds to clinical assessment.

Shimazu et al. observed the discharge patterns of the same single neuromuscular unit of the biceps brachii muscle with Parkinsonian rigidity on electromyography [9]. Their results suggest that a reduced spike-to-spike interval in rigidity tends to increase in the course of pallidotomy. It is possible that the decreased spike-to-spike interval in rigidity occurred because of not only overactivation of tonic motor units, but also a change to tonic in the phasic motor units as a result of excessive activity of afferent fibers from the muscle spindle. This interpretation is based on the report of Granit et al., who demonstrated that phasic alpha motor neurons show an increased stretch reflex and tonic properties during periods of excessive muscle spindle activity with the injection of succinylcholine [10].

Rothwell et al. demonstrated that the long latency stretch reflex in triceps brachii in PD patients with severe rigidity showed a larger response than normal controls, whereas a normal response was observed in flexor pollicis longus [4]. They also showed that the M2 response in flexor pollicis longus in PD patients with severe rigidity increased with

velocity, although saturation occurred at velocities greater than $300^\circ/\text{s}$. In clinical examinations, rigidity is detected by passive movement in the main joint, and the physician cannot move the joint at a high speed over $300^\circ/\text{s}$. Moreover, it is hard for the examiner to assess the rigidity in flexor pollicis longus in such a small joint. The velocity-dependent component of Parkinsonian rigidity in the elbow joint may be derived from an exaggerated long latency stretch reflex.

Using this measurement system, we previously reported that Parkinsonian rigidity varies with joint angle [7]. Those findings, together with the present results, suggest that the features of rigidity may not conform to the conventional definition that rigidity is constant regardless of joint angle and does not depend on the speed at which the joint is moved. Differences in bias are high in subjects with a UPDRS rigidity score of 2 or greater. It may be said that physicians can feel velocity-dependency in some patients with moderate to severe rigidity because they evaluate rigidity as a combination of two components: the elastic coefficient and differences in bias.

Detailed analysis of spasticity using this technique may open the way to development of a unified model of muscle tone abnormality in neurological diseases.

Conflict of Interests

The authors declare that there is no conflict of interests regarding the publication of this paper.

Acknowledgments

The authors would like to thank Dr. Toshimitsu Hamasaki (Department of Medical Statistics, Osaka University Graduate School of Medicine) for his assistance in the statistical analysis. This study was supported by the Program for

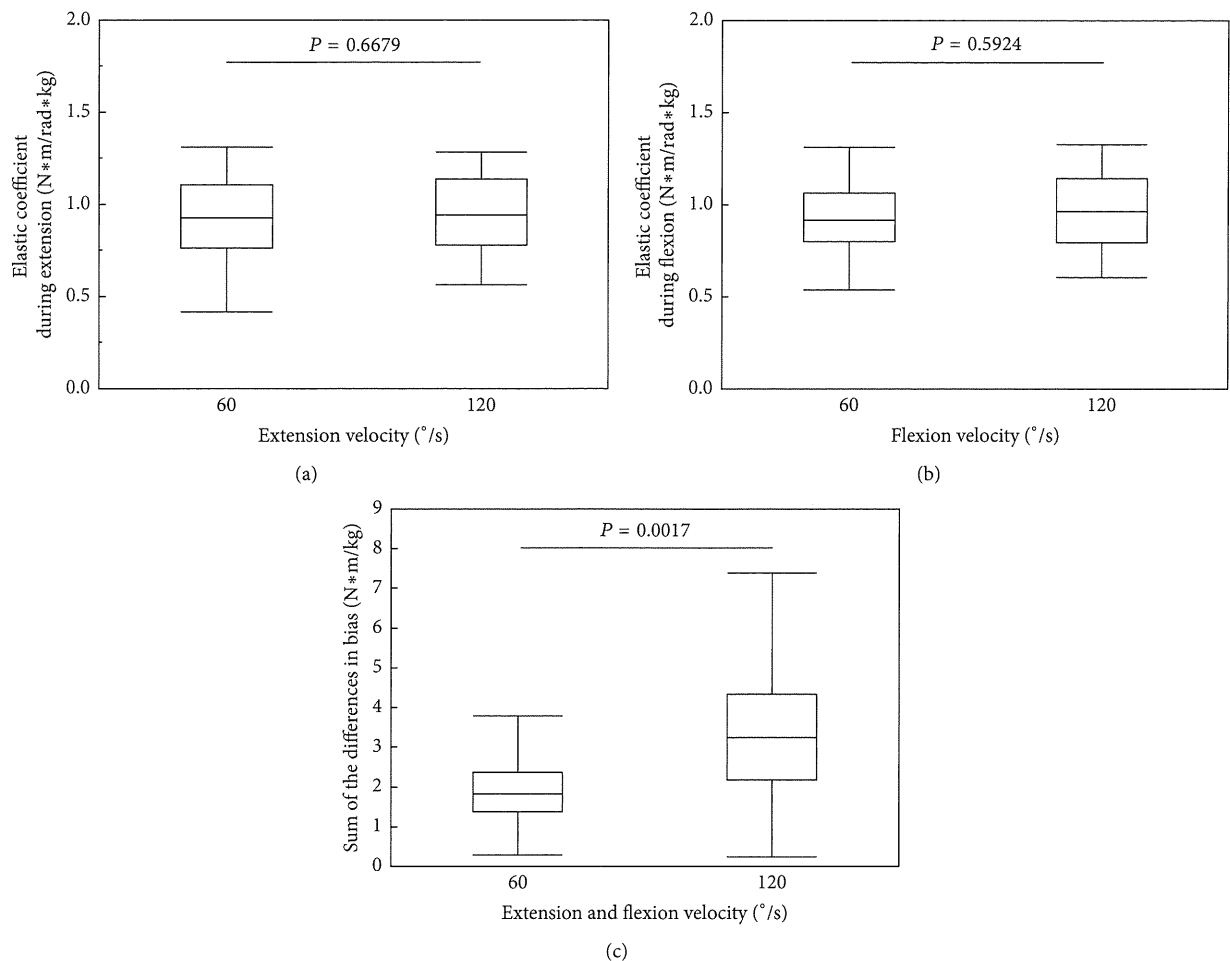


FIGURE 3: Changes in the (a) elastic coefficient during elbow extension, (b) elastic coefficient during elbow flexion, and (c) sum of the difference in bias with changes in extension and flexion velocity.

Promotion of Fundamental Studies in Health Sciences of the National Institute of Biomedical Innovation (NIBIO). This work was supported by JSPS KAKENHI 23700551.

References

- [1] J. Shahed and J. Jankovic, "Motor symptoms in Parkinson's disease," *Handbook of Clinical Neurology*, vol. 83, pp. 329–342, 2007.
- [2] H.-M. Lee, Y.-Z. Huang, J.-J. Chen, and I.-S. Hwang, "Quantitative analysis of the velocity related pathophysiology of spasticity and rigidity in the elbow flexors," *Journal of Neurology Neurosurgery and Psychiatry*, vol. 72, no. 5, pp. 621–629, 2002.
- [3] R. G. Lee and W. G. Tatton, "Motor responses to sudden limb displacements in primates with specific CNS lesions and in human patients with motor system disorders," *Canadian Journal of Neurological Sciences*, vol. 2, no. 3, pp. 285–293, 1975.
- [4] J. C. Rothwell, J. A. Obeso, M. M. Traub, and C. D. Marsden, "The behaviour of the long-latency stretch reflex in patients with Parkinson's disease," *Journal of Neurology Neurosurgery and Psychiatry*, vol. 46, no. 1, pp. 35–44, 1983.
- [5] M. A. Relja, D. Petracic, and M. Kolaj, "Quantifying rigidity with a new computerized elbow device," *Clinical Neuropharmacology*, vol. 19, no. 2, pp. 148–156, 1996.
- [6] T. Endo, R. Okuno, M. Yokoe, K. Akazawa, and S. Sakoda, "A novel method for systematic analysis of rigidity in Parkinson's disease," *Movement Disorders*, vol. 24, no. 15, pp. 2218–2224, 2009.
- [7] T. Endo, T. Hamasaki, R. Okuno et al., "Parkinsonian rigidity shows variable properties depending on the elbow joint angle," *Parkinson's Disease*, vol. 2013, Article ID 258374, 5 pages, 2013.
- [8] W. R. G. Gibb and A. J. Lees, "The relevance of the Lewy body to the pathogenesis of idiopathic Parkinson's disease," *Journal of Neurology, Neurosurgery and Psychiatry*, vol. 51, no. 6, pp. 745–752, 1988.
- [9] H. Shimazu, T. Hongo, K. Kubota, and H. Narabayashi, "Rigidity and spasticity in man. Electromyographic analysis with reference to the role of the globus pallidus," *Archives of Neurology*, vol. 6, no. 1, pp. 10–17, 1962.
- [10] R. Granit, S. Skoglund, and S. Thesleff, "The action of succinylcholine and curare on the muscle spindles," *Acta Physiologica Scandinavica*, vol. 29, no. 1, p. 86, 1953.

Survivin expression in lung cancer: Association with smoking, histological types and pathological stages

HIROSHI HIRANO¹, HAJIME MAEDA², TOSHIHIKO YAMAGUCHI³,
SOICHIRO YOKOTA³, MASAHIDE MORI³ and SABURO SAKODA³

Departments of ¹Pathology, ²Surgery and ³Internal Medicine, Toneyama National Hospital, Toyonaka, Osaka 560-8552, Japan

Received July 14, 2014; Accepted April 14, 2015

DOI: 10.3892/ol.2015.3374

Abstract. Survivin is expressed in the nucleus and/or cytoplasm of various malignant cells. Nuclear survivin is critical for the completion of mitosis, while cytoplasmic survivin functions as an inhibitor of apoptosis. The expression of survivin has been reported to be associated with the aggressiveness of certain types of cancer. The present study examined the association between cigarette smoking history and the expression of survivin and Ki-67 in lung adenocarcinomas of pathological (p) stages I, II and III. The expression of survivin and Ki-67 in adenocarcinomas was also compared with that of other p-stage I lung cancers, including squamous cell carcinoma (SqCC), large cell neuroendocrine carcinoma (LCNEC) and small cell carcinoma (SmCCs), of patients with a smoking history. In adenocarcinomas at p-stage I, labeling indices (LIs) of nuclear survivin and Ki-67 were significantly higher in tissue samples from smokers than those from non-smokers; however, the nuclear survivin and Ki-67 LIs in p-stage II and III adenocarcinomas from non-smokers and smokers were similar to those in p-stage I adenocarcinomas of smokers. The nuclear survivin and Ki-67 LIs in adenocarcinomas of smokers at p-stage I were lower than those in SqCCs, LCNECs and SmCCs of smokers at the same stage. Smokers with adenocarcinoma also exhibited a higher survival rate compared with that of smokers with SqCCs, LCNECs and SmCCs. The present results indicated that a history of smoking is associated with increased nuclear survivin and Ki-67 expression in lung adenocarcinomas of p-stage I, but not p-stages II or III. In

addition it was revealed that, in smokers, the nuclear survivin and Ki-67 expression in p-stage I adenocarcinomas was lower than that of other p-stage I lung cancer types, and was associated with an enhanced survival rate. In conclusion, smoking is associated with the histogenesis of lung adenocarcinoma but not with the development of lung adenocarcinoma, based on the nuclear expression levels of Ki-67 and survivin.

Introduction

Survivin was first identified in 1997 as a member of the inhibitor of apoptosis protein (IAP) family, which contain a family-specific baculovirus IAP repeat (BIR) (1). This BIR domain exists at the N-terminal and is associated with the inhibition of apoptosis (2). The human survivin gene is located on chromosome 17 (17q25) (3). Survivin is expressed in the nucleus and/or cytoplasm of various malignant tumor cells (4), and is also expressed in fetal and certain proliferating adult tissues, although remains undetectable in differentiated tissues (5). In the cytoplasm, survivin functions as an inhibitor of apoptosis, while in the nucleus, survivin regulates cell proliferation (6).

Survivin possesses a nuclear export signal (NES), which allows it to bind to its export receptor, chromosome region maintenance protein 1 (Crm1). In the nucleus, survivin forms a complex with aurora kinase B, the inner centromere protein (INCENP) and borealin to complete mitosis. Crm1 is critical in tethering this complex to the centromere (Fig. 1) (7). At the end of mitosis, Crm1 is released from this complex and exports survivin from the nucleus to the cytoplasm, where it functions as an inhibitor of apoptosis.

Human survivin has multiple splice variants, which have various functions and localizations; wild type survivin (WT-survivin), survivin-2a, survivin-2B, survivin-ΔEx3 and survivin-3B have been identified to date (Fig. 2) (8). Survivin-ΔEx3 and survivin-2a lack a nuclear localization signal (NLS), and remain in the cytoplasm, while WT-survivin, survivin-2B and survivin-3B possess an NLS and are able to function in the completion of mitosis in the nucleus (9).

Various types of cancer express survivin. As survivin has a dual role as an apoptosis inhibitor and a mitotic effector, the expression of survivin in cancer cells may protect them from therapeutic drug-induced apoptosis and promote their proliferation. The association between the aggressiveness of

Correspondence to: Dr Hiroshi Hirano, Department of Pathology, Toneyama National Hospital, 1-1, Toneyama 5 chome, Toyonaka, Osaka 560-8552, Japan
E-mail: hi-hi-hirano@hotmail.com

Abbreviations: IAP, inhibitor of apoptosis protein; BIR, baculovirus IAP repeat; NES, nuclear export signal; NLS, nuclear localization signal; Crm1, chromosome region maintenance protein 1; INCENP, inner centromere protein; SqCC, squamous cell carcinoma; LCNEC, large cell neuroendocrine carcinoma; SmCC, small cell carcinoma.

Key words: survivin, lung cancer, smoking, histological type, Ki-67

cancer cells and the expression of survivin has been investigated in numerous types of cancer (10-12). However, various studies have reported inconsistent findings with regard to the significance of survivin as a prognostic factor for cancer patients. Nuclear survivin expression has been reported to be correlated with poor prognosis in patients with various types of cancer, including hepatocellular carcinoma, esophageal squamous cell carcinoma, as well as urinary bladder and ovarian cancer (12-15). However, it has been reported to be a valuable prognostic factor in other types of cancer, for example gastric cancer and invasive breast cancer (10,16). With regard to lung cancer, nuclear survivin expression has been reported to be a useful prognostic factor for patients with advanced non-small cell cancers (stages III and IV), and a poor prognostic factor for patients with non-small cell carcinomas at earlier stages (I and II). Although a number of studies have investigated survivin expression in non-small cell lung carcinomas (11,17,18), little data is available with regard to survivin expression in lung cancers of various histological types at various stages, or the association between survivin expression and smoking history. The paraffin-embedded blocks of lung tumor tissue removed during surgeries performed in Toneyama National Hospital (Toyonaka, Osaka, Japan) between 2002 and 2011 included sufficient numbers to allow statistical analysis of adenocarcinomas from smokers and non-smokers at p-stages I, II and III, as well as squamous cell carcinomas (SqCCs), large cell neuroendocrine carcinomas (LCNECs) and small cell carcinomas (SmCCs) from smokers at p-stage I. Among the proliferative markers of tumors, the Ki-67 labeling index (Ki67-LI) is widely accepted as one of the most reliable markers for estimating the malignancy grade and the prognosis of various types of tumor (19). The Ki-67 LI of non-small cell lung carcinoma has prognostic value (20). The present study investigated the expression of survivin and Ki-67 in these tumors.

Materials and methods

Patients and specimens. Paraffin-embedded tissue blocks of adenocarcinomas of p-stages I, II and III, as well as SqCCs, LCNECs and SmCCs at p-stage I, were selected. All tissues were obtained during surgeries performed at Toneyama National Hospital (Osaka, Japan) from January 2002 to December 2011. None of the patients whose tissues were used in the present study had received chemotherapy or radiotherapy prior to surgery. The numbers of samples obtained are presented in Table I. The Brinkman index (BI), which is described in Table I represents the number of pieces of tobacco smoked/day, multiplied by the number of years smoking history. The mortality of lung cancer patients with a BI ≥ 400 is ~ 4.9 times higher compared with that of non-smoking patients (21). In the present study, the majority of the patients with SqCC, LCNEC and SmCC had a high BI, and the poor prognosis of those histological types is possibly due to an increased BI. The adenocarcinoma samples were almost evenly distributed between p-stages I, II and III, and were identified in non-smokers and smokers (including current smokers and ex-smokers) (Table I). By contrast, the majority of SqCCs, LCNECs and SmCCs were of p-stage I and almost all patients who had

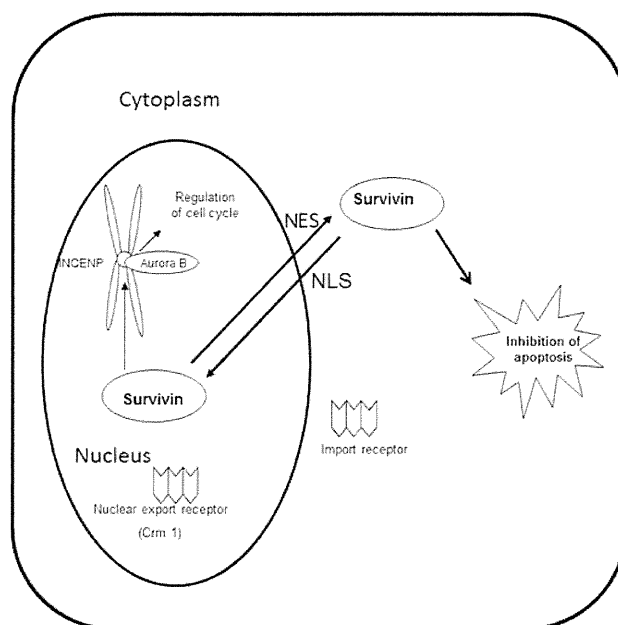


Figure 1. Functions, localization and transport of survivin. INCENP, inner centromere protein; NES, nuclear export signal; NLS, nuclear localization signal; Crm1, chromosome region maintenance protein 1.

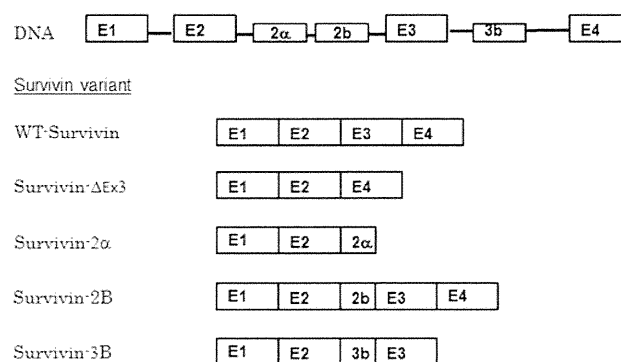


Figure 2. Human survivin splice variants. E, exon; WT, wild type.

undergone surgery for these types of tumor were smokers (Table I).

The paraffin-embedded tissue blocks used for this study were produced following the fixation of tumor tissues in 0.01 M phosphate-buffered 10% formalin (pH 7.4). Clinical data, including follow-up findings, were available for all cases. Written informed consent from each patient, allowing the arbitrary use of tumor tissues for pathological studies, was obtained prior to surgery. The present study was approved by the ethics committee of Toneyama National Hospital (approval number 1334).

Immunohistochemistry. For immunohistochemical examinations of survivin, one representative tissue block from each tumor was used, with 5-mm sections prepared. Immunohistochemical staining was performed using an avidin-streptavidin immunoperoxidase method with a rabbit polyclonal anti-human survivin antibody (Novus Biologicals,

Table I. Clinical features of patients with various subtypes of lung cancer.

A, Adenocarcinoma (n=87)				
Characteristic	Stage I	Stage II	Stage III	
Patients, n	34	22	31	
Age, years				
Mean \pm SE	66.4 \pm 1.5	66.6 \pm 1.8	65.8 \pm 1.2	
Range	50-80	53-80	47-81	
Gender, n				
Male	20	15	18	
Female	14	7	13	
Smoking status, n				
Non-smoker	13	4	8	
Smoker	21	18	23	
BI of smoker, mean \pm SE	921.2 \pm 57.5	829.2 \pm 108.0	1137.6 \pm 137.9	
B, Squamous cell carcinoma (n=44)				
Characteristic	Stage I	Stage II	Stage III	
Patients, n	33	2	9	
Age, years				
Mean \pm SE	68.4 \pm 1.5	66.5 \pm 7.6	70.9 \pm 3.4	
Range	55-79	59-74	48-82	
Gender, n				
Male	30	2	7	
Female	3	1	2	
Smoking status, n				
Non-smoker	1	0	1	
Smoker	32	2	8	
BI of smoker, mean \pm SE	1179.4 \pm 83.7		935.6 \pm 231.1	
C, Large cell neuroendocrine carcinoma (n=13)				
Characteristic	Stage I	Stage II	Stage III	
Patients, n	13	0	0	
Age, years				
Mean \pm SE	69.3 \pm 2.8			
Range	58-79			
Gender, n				
Male	12			
Female	1			
Smoking status, n				
Non-smoker	1			
Smoker	12			
BI of smoker, mean \pm SE	1012.9 \pm 118.0			
D, Small cell carcinoma (n=13)				
Characteristic	Stage I	Stage II	Stage III	
Patients, n	10	2	1	

Table I. Continued.

Characteristic	Stage I	Stage II	Stage III
Age, years			
Mean \pm SE	69.1 \pm 2.9		
Range	56-79	62-73	80
Gender, n			
Male	9	2	0
Female	1	1	1
Smoking status, n			
Non-smoker	0	0	0
Smoker	10	2	1
BI of smoker, mean \pm SEM	948 \pm 127.4		

SE, standard error of the mean; BI, Brinkman index.

Table II. Survivin expression and Ki-67 labeling indices in adenocarcinomas of non-smokers and smokers at p-stage I, II or III.

Stage	Non-smokers	Smokers	Difference
Stage I, n	13	21	
Survivin nuclear labeling index, %	2.9 \pm 1.0	9.7 \pm 2.4	P<0.05
Survivin cytoplasm expression >10%, n (%)	12 (92.3)	16 (76.2)	NS
Ki-67 labeling index, %	12.0 \pm 1.6	20.5 \pm 2.8	P<0.05
Stage II, n	4	18	
Survivin nuclear labeling index, %	9.0 \pm 2.7	12.3 \pm 2.1	NS
Survivin cytoplasm expression >10%, n (%)	3 (75.0)	9 (50.0)	NS
Ki-67 labeling index, %	17.8 \pm 4.5	28.1 \pm 3.3	NS
Stage III, n	8	23	
Survivin nuclear labeling index, %	7.1 \pm 1.8	13.2 \pm 2.8	NS
Survivin cytoplasm expression >10%, n (%)	7 (87.5)	12 (52.2)	NS
Ki-67 labeling index, %	15.1 \pm 2.6	21.9 \pm 2.1	NS

Nuclear survivin and Ki-67 labeling indices are presented as the mean \pm standard error of the mean. NS, not significant.

Littleton, CO, USA) at a 1:500 dilution, or with a prediluted anti-human Ki-67 mouse monoclonal antibody (Dako, Glostrup, Denmark). The primary antibodies were detected using the iView DAB universal kit (Ventana Medical Systems Inc., Tucson, AZ, USA), which is a detection kit including from a mixture of anti-mouse Ig and anti-rabbit Ig biotinylated secondary antibodies using DAB/H₂O₂ as substrates. Antigen retrieval was conducted by incubation of deparaffinized sections in cell condition 1 solution from the aforementioned kit for 64 min at 100°C and immunohistochemical staining was conducted using an automated Benchmark system (Ventana Medical System, Tuscon, AZ, USA), according to the manufacturer's instructions. To estimate the labeling index (LI) of nuclear survivin or Ki-67 in each tumor, ~1,000 nuclei stained positively or negatively were counted automatically, using Win Roof software (Mitani Co, Tokyo, Japan). To determine positive staining of cytoplasmic survivin, tumors were classified into two groups based on the percentage of

positively stained cells: >10%, positive staining; and <10%, negative staining.

Statistical analysis. Statistical analyses were performed using the Excel Statistics 2012 software package for Windows (SSRI, Tokyo, Japan). P<0.05 was considered to indicate a statistically significant difference. Categorical data was analyzed using a χ^2 test. Data comprising multiple values are presented as the mean \pm standard error of the mean and these data were analyzed using Bonferroni's multiple comparison test. The survival curves were analyzed by the Kaplan-Meier method, followed by the Log rank test.

Results

Survivin expression in adenocarcinomas of non-smokers and smokers. In adenocarcinomas at p-stage I, the nuclear survivin LIs were significantly higher for smokers than for non-smokers

Table III. Survivin expression and Ki-67 labeling indices in various histological types of lung cancer in smokers.

Stage	Adenocarcinoma	SqCC	LCNEC	SmCC
Stage I, n	21	32	12	10
Survivin nuclear labeling index, %	9.7±2.4 ^{b,c,d}	29.1±2.9 ^{a,c}	41.5±2.3 ^{a,b}	33.3±3.2 ^a
Survivin cytoplasm expression >10%, n (%)	16 (76.2) ^{c,d}	29 (90.6) ^{c,d}	3 (25.0) ^{a,b}	3 (30.0) ^{a,b}
Ki-67 labeling index, %	20.5±2.8 ^{b,c,d}	45.5±2.7 ^a	46.9±7.4 ^a	54.2±4.0 ^a
Stage III, n	23	8		
Survivin nuclear labeling index, %	13.2±2.8	19.4±4.2		
Survivin cytoplasm expression >10%, n (%)	12 (52.2)	7 (87.5)		
Ki-67 labeling index, %	21.9±2.1 ^b	32.2±4.5 ^a		

SqCC, squamous cell carcinoma; LCNEC, large cell neuroendocrine carcinoma; SmCC, small cell carcinoma. Nuclear survivin and Ki-67 labeling indices are presented as the mean ± standard error of the mean. ^aP<0.05 vs. adenocarcinoma; ^bP<0.05 vs. SqCC; ^cP<0.05 vs. LCNEC; ^dP<0.05 vs. SmCC.

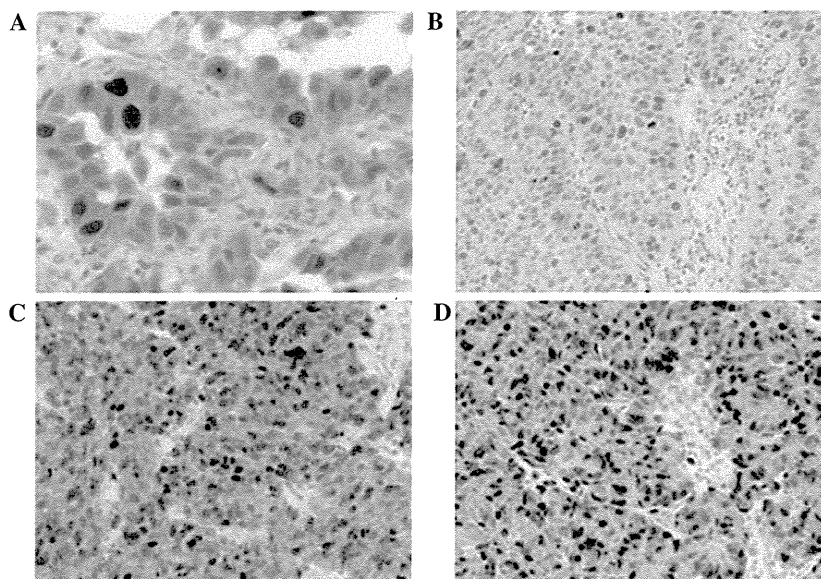


Figure 3. Immunohistochemical staining of survivin in p-stage I lung carcinomas: (A) Nuclear and cytoplasmic expression in adenocarcinoma (x40 magnification); (B) nuclear expression in squamous cell carcinoma (x20 magnification); (C) nuclear expression in small cell carcinoma (x20 magnification); (D) nuclear expression in large cell neuroendocrine carcinoma (x20 magnification).

(P<0.05), while there was no significant difference in the cytoplasmic survivin expression between adenocarcinomas from smokers and non-smokers (Table II; Fig. 3A). The Ki-67 LIs of the adenocarcinomas of smokers were also significantly higher compared with those of the adenocarcinomas of non-smokers. In adenocarcinomas at p-stage II and III, smoking history was not significantly associated with the nuclear survivin LI, cytoplasmic survivin expression or Ki-67 LI. The nuclear survivin LIs and Ki-67 LIs in adenocarcinomas at p-stage II and III were similar to those in adenocarcinomas of smokers at p-stage I.

Survivin expression in lung cancers of various histological types. Survivin expression and Ki-67 LIs were compared between adenocarcinomas and other histological types of lung carcinoma, including SqCC, LCNEC and SmCC, from smokers at p-stage I, as almost all patients who had undergone

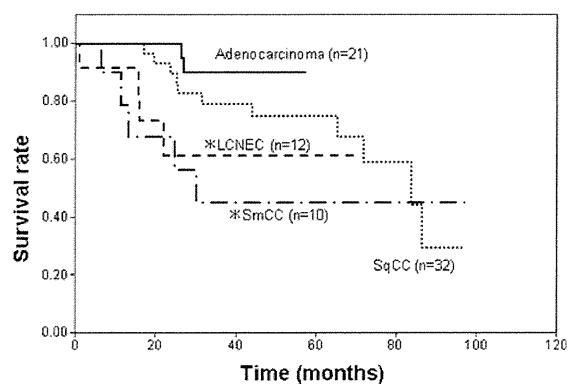


Figure 4. Survival curves of patients with a history of smoking with various histological types of lung carcinoma at p-stage I. LCNEC, large cell neuroendocrine carcinoma; SmCC, small cell carcinoma; SqCC, squamous cell carcinoma. *P<0.05 vs. adenocarcinoma.

surgery for the treatment of SqCC, LCNEC and SmCC were smokers (Table II). The nuclear survivin and Ki-67 LIs in the adenocarcinoma samples were significantly lower compared with those of the SqCC, LCNEC and SmCC samples ($P < 0.05$; Table III; Fig. 3B, C and D). By contrast, the cytoplasmic survivin expression in SqCC samples was similar to that of adenocarcinoma samples, whilst it was decreased in LCNEC and SmCC compared with adenocarcinoma.

Survival rate of patients with different histological types of lung carcinoma. When the survival rates were compared among smokers with adenocarcinoma, SqCC, LCNEC and SmCC at p-stage I, the survival rates of smokers with LCNEC and SmCC were significantly poorer compared with that of smokers with adenocarcinoma (Fig. 4). The survival rate of SqCC patients was also poorer than that of adenocarcinoma patients, however, this difference was not statistically significant. The duration of the follow-up for the p-stage I adenocarcinoma patients was shorter compared with the other type of lung carcinoma patients, since p-stage I adenocarcinoma has a more favorable prognosis; therefore, a 5-year follow-up was considered to be sufficient.

In conclusion, the present study indicates that smoking is associated with the histogenesis of lung adenocarcinoma but not with the development of lung adenocarcinoma, based on the nuclear expression levels of Ki-67 and survivin in lung cancer tissue samples.

Discussion

In adenocarcinomas at p-stage I, the LIs of nuclear survivin and Ki-67 were significantly higher in the adenocarcinomas of smokers than in adenocarcinomas of non-smokers. These results are consistent with the results of a previous study by our group, in which an association was identified between smoking and nuclear survivin expression and Ki-67 LI in p-stage IA adenocarcinomas (18). Dasgupta *et al* (22) have reported that the cigarette component nicotine upregulates survivin expression in human non-small cell carcinoma cell lines. Therefore, it is conceivable that smoking induces survivin expression at an early developmental stage of lung adenocarcinoma. The increased nuclear survivin expression in the adenocarcinomas of smokers compared with that of non-smokers may be associated with the higher Ki-67 LIs in these adenocarcinomas. Maeda *et al* (23) reported that smoking was associated with poor outcomes in patients with clinical stage IA adenocarcinomas. The poor prognoses of these patients may be associated with the increased nuclear survivin expression.

Notably, nuclear survivin and Ki-67 LIs, in adenocarcinomas at p-stages II and III of non-smokers and smokers were similar to those in p-stage I adenocarcinomas of smokers. These results indicate that nuclear survivin expression and proliferative activity may be increased during the progression of disease following the early developmental stages of adenocarcinoma.

Nuclear survivin and Ki-67 LIs in adenocarcinomas of smokers at p-stage I were significantly lower compared with those of SqCCs, LCNECs and SmCCs of smokers at the same stage. These results suggested that survivin expression may depend on the histological type of lung cancer, at least at p-stage I. The higher Ki-67 LIs in SqCCs, LCNECs and SmCCs may be associated with higher nuclear survivin expression in

these histological types of lung cancer. Inconsistent with the higher Ki-67 LIs in SqCCs, LCNECs and SmCCs compared with that of adenocarcinomas of smokers at p-stage I, the survival rates of smokers with SqCCs, LCNECs and SmCCs were poorer than those of smokers with adenocarcinoma.

In contrast to the nuclear expression of survivin, cytoplasmic survivin expression was not increased in non-adenocarcinoma lung cancer types compared with that in adenocarcinoma, and the poorer survival rates of patients with these types of cancer were not associated with its increase. Therefore, cytoplasmic survivin expression may have little effect on the proliferation or prognosis of lung cancer.

In conclusion, the present results suggest that a history of smoking is accompanied by an increase in nuclear survivin and Ki-67 expression in lung adenocarcinomas at p-stage I, but not at p-stage II and III; and that nuclear survivin and Ki-67 expression in adenocarcinomas of smokers at p-stage I is lower than that in other types of lung cancer of smokers at p-stage I, which is associated with an enhanced survival rate.

Acknowledgements

The authors would like to thank Mr. Akira Kimura and Mr. Hiroshi Yamada (Laboratory Medicine, Toneyama National Hospital) for their technical assistance, and Ms. Yuko Ito (Laboratory Medicine, Toneyama National Hospital) for providing secretarial assistance.

References

1. Ambrosini G, Adida C and Altieri DC: A novel anti-apoptosis gene, survivin, expressed in cancer and lymphoma. *Nat Med* 3: 917-921, 1997.
2. Srinivasula SM and Ashwell JD: IAPs: What's in a name? *Mol Cell* 30: 123-135, 2008.
3. Storlazzi CT, Brekke HR, Mandahl N, *et al*: Identification of a novel amplicon at distal 17q containing the BIRC5/SURVIVIN gene in malignant peripheral nerve sheath tumours. *J Pathol* 209: 492-500, 2006.
4. Connell CM, Colnaghi R and Wheatley SP: Nuclear survivin has reduced stability and is not cytoprotective. *J Biol Chem* 283: 3289-3296, 2008.
5. Salvesen GS and Duckett CS: IAP proteins: Blocking the road to death's door. *Nat Rev Mol Cell Biol* 3: 401-410, 2002.
6. Stauber RH, Mann W and Knauer SK: Nuclear and cytoplasmic survivin: Molecular mechanism, prognostic, and therapeutic potential. *Cancer Res* 67: 5999-6002, 2007.
7. Knauer SK, Mann W and Stauber RH: Survivin's dual role: An export's view. *Cell Cycle* 6: 518-521, 2007.
8. Mull AN, Klar A and Navara CS: Differential localization and high expression of SURVIVIN splice variants in human embryonic stem cells but not in differentiated cells implicate a role for SURVIVIN in pluripotency. *Stem Cell Res (Amst)* 12: 539-549, 2014.
9. Li F and Ling X: Survivin study: An update of 'What is the next wave'? *J Cell Physiol* 208: 476-486, 2006.
10. Hernandez JM, Farma JM, Coppola D, *et al*: Expression of the antiapoptotic protein survivin in colon cancer. *Clin Colorectal Cancer* 10: 188-193, 2011.
11. Xie YL, An L, Jiang H and Wang J: Nuclear survivin expression is associated with a poor prognosis in Caucasian non-small cell lung cancer patients. *Clin Chim Acta* 414: 41-43, 2012.
12. Vivas-Mejia PE, Rodriguez-Aguayo C, Han HD, *et al*: Silencing survivin splice variant 2B leads to antitumor activity in taxane-resistant ovarian cancer. *Clin Cancer Res* 17: 3716-3726, 2011.
13. Morinaga S, Nakamura Y, Ishiwa N, *et al*: Expression of survivin mRNA associates with apoptosis, proliferation and histologically aggressive features in hepatocellular carcinoma. *Oncol Rep* 12: 1189-1194, 2004.

14. Zhu H, Wang Q, Hu C, *et al*: High expression of survivin predicts poor prognosis in esophageal squamous cell carcinoma following radiotherapy. *Tumour Biol* 32: 1147-1153, 2011.
15. Sun YW, Xuan Q, Shu QA, *et al*: Correlation of tumor relapse and elevated expression of survivin and vascular endothelial growth factor in superficial bladder transitional cell carcinoma. *Genet Mol Res* 12: 1045-1053, 2013.
16. Vallböhmer D, Drebber U, Schneider PM, *et al*: Survivin expression in gastric cancer: Association with histomorphological response to neoadjuvant therapy and prognosis. *J Surg Oncol* 99: 409-413, 2009.
17. Ichiki Y, Hanagiri T, Takenoyama M, *et al*: Tumor specific expression of survivin-2B in lung cancer as a novel target of immunotherapy. *Lung Cancer* 48: 281-289, 2005.
18. Hirano H, Maeda H, Takeuchi Y, *et al*: Association of cigarette smoking with the expression of nuclear survivin in pathological Stage IA lung adenocarcinomas. *Med Mol Morphol* 47: 196-200, 2014.
19. Gerdes J, Schwab U, Lemke H and Stein H: Production of a mouse monoclonal antibody reactive with a nuclear antigen associated with cell proliferation. *Int J Cancer* 31: 13-20, 1983.
20. Nguyen VN, Mirejovský P, Mirejovský T, *et al*: Expression of cyclin D1, Ki-67 and PCNA in non-small cell lung cancer: Prognostic significance and comparison with p53 and bcl-2. *Acta Histochem* 102: 323-338, 2000.
21. Maeshima AM, Tochigi N, Tsuta K, *et al*: Histological evaluation of the effect of smoking on peripheral small adenocarcinomas of the lung. *J Thorac Oncol* 3: 698-703, 2008.
22. Dasgupta P, Kinkade R, Joshi B, *et al*: Nicotine inhibits apoptosis induced by chemotherapeutic drugs by up-regulating XIAP and survivin. *Proc Natl Acad Sci USA* 103: 6332-6337, 2006.
23. Maeda R, Yoshida J, Ishii G, *et al*: Influence of cigarette smoking on survival and tumor invasiveness in clinical stage IA lung adenocarcinoma. *Ann Thorac Surg* 93: 1626-1632, 2012.